JNS Atlas
CLINICAL ARTICLE
J Neurosurg 137:609–617, 2022

Dumbbell-shaped pituitary adenomas: prognostic factors for prediction of tumor nondescent of the supradiaphragmal component from a multicenter series

*Alexander S. G. Micko, MD, PhD,[1] Omar Keritam, MD,[1] Wolfgang Marik, MD,[2] Ben A. Strickland, MD,[3] Robert G. Briggs, MD,[3] Shane Shahrestani, PhD,[3] Tyler Cardinal, MD,[3] Engelbert Knosp, MD,[1] Gabriel Zada, MD,[3] and Stefan Wolfsberger, MD[1]

[1]Department of Neurosurgery, Medical University of Vienna; [2]Department of Biomedical Imaging and Image-guided Therapy, Division of Neuroradiology and Musculoskeletal Radiology, Medical University of Vienna, Austria; and [3]Department of Neurological Surgery, Keck School of Medicine, University of Southern California, Los Angeles, California

OBJECTIVE Dumbbell-shaped pituitary adenomas (DSPAs) are a subgroup of macroadenomas with suprasellar extension that are characterized by a smaller diameter at the level of the diaphragma sellae opening compared with the supradiaphragmal tumor component (SDTC). Hence, DSPAs may be particularly prone to a nondescending suprasellar tumor component and risk for residual tumor or postoperative bleeding.

METHODS A multicenter retrospective cohort analysis of 99 patients with DSPA operated on via direct endoscopic endonasal transsphenoidal approach between 2011 and 2020 was conducted. Patient recruitment was performed at two tertiary care centers (Medical University of Vienna and University of Southern California) with expertise in endoscopic skull base surgery. DSPA was defined as having a smaller diameter at the level of the diaphragma sellae compared with the SDTC.

RESULTS On preoperative MRI, all DSPAs were macroadenomas (maximum diameter range 17–71 mm, volume range 2–88 cm^3). Tumor descent was found in 73 (74%) of 99 patients (group A), and nondescent in 26 (26%) of 99 patients (group B) intraoperatively. DSPAs in group A had a significantly smaller diameter (30 vs 42 mm, $p < 0.001$) and significantly smaller volume (10 vs 22 cm^3, $p < 0.001$) than those in group B. The ratio of the minimum area at the level of the diaphragmal opening in comparison with the maximum area of the suprasellar tumor component ("neck-to-dome area") was significantly lower in group A than in group B (1.7 vs 2.7, $p < 0.001$). Receiver operating characteristic curve analysis revealed an area under the curve of 0.75 (95% CI 0.63–0.87). At a cutoff ratio of 1.9, the sensitivity and specificity for a nondescending suprasellar tumor component were 77% and 34%, respectively.

CONCLUSIONS In the present study, the neck-to-dome area ratio was of prognostic value for prediction of intraoperative tumor nondescent in DSPAs operated on via a direct endonasal endoscopic approach. Pituitary adenoma SDTC nondescent carried the inherent risk of hemorrhagic transformation in all cases.

https://thejns.org/doi/abs/10.3171/2021.9.JNS211689

KEYWORDS dumbbell-shaped; pituitary adenoma; endoscopic; prognosis; pituitary surgery

The standard (direct) endonasal transsphenoidal approach has become the mainstay for removal of most pituitary adenomas, even those with suprasellar extension.[1–5] Although these tumors are approached from below, the majority of the supradiaphragmal tumor component (SDTC) will descend into the sella after removal of the infradiaphragmal tumor component (IDTC), either spontaneously or after different methods to increase intracranial pressure (e.g., jugular vein compression, Valsalva maneuver, and elevated positive end-expiratory pressure).[6,7] However, a considerable proportion of the SDTC of the pituitary adenoma does not descend intraoperatively and has been attributed to various factors, including adherence to neurovascular structures, tumor consistency, and

ABBREVIATIONS AComA = anterior communicating artery; DSPA = dumbbell-shaped pituitary adenoma; GTR = gross-total resection; IDTC = infradiaphragmal tumor component; ROC = receiver operating characteristic; SDTC = supradiaphragmal tumor component.

SUBMITTED July 7, 2021. **ACCEPTED** September 28, 2021.
INCLUDE WHEN CITING Published online December 24, 2021; DOI: 10.3171/2021.9.JNS211689.

* G.Z. and S.W. contributed equally to this work.

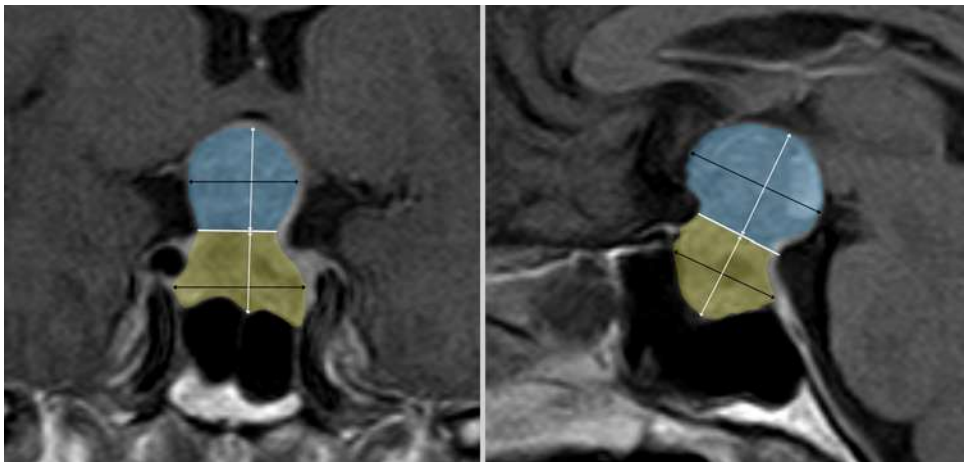

FIG. 1. MRI sequence analysis. Coronal (**left**) and sagittal (**right**) views of the DSPA. The *yellow shaded areas* demonstrate the IDTC, and the *blue shaded areas* demonstrate the SDTC. The *white arrows* designate the maximum tumor height (infra- and supradiaphragmal); *white lines*, the diaphragmal area; and *black arrows*, the maximum tumor width (infra- and supradiaphragmal). Figure is available in color online only.

hourglass narrowing of the pituitary adenoma at the level of the diaphragma sellae.[7–10]

Dumbbell-shaped pituitary adenomas (DSPAs) are a subgroup of pituitary macroadenomas with suprasellar extension that are defined by a smaller diameter at the level of the diaphragma sellae opening than at the level of the SDTC. The resulting shape of the tumor resembles a dumbbell or hourglass, which is a classic descriptor for many nonfunctional pituitary adenomas.[11] Hence, DSPAs may be particularly prone to not descending due to their configuration and commonly large SDTC. Surgical limitations of tumor removal may be attributed to the fact that pulling of the tumor is contraindicated and carries the risk of uncontrollable suprasellar hemorrhage. A possible consideration is conversion to an extended (e.g., transtuberculum) approach when needed. The risk of subtotal resection of the SDTC carries the reported potential for postoperative bleeding and vision loss.[12]

Therefore, preoperative knowledge about the risk of a nondescending SDTC is critical when discussing the surgical strategy with the patient and designing the approach appropriately (e.g., nasoseptal flap, turbinectomy, posterior ethmoidectomy, extended approach, and lumbar drain). Criteria for tumor descent to assess different approaches are necessary but have not been systematically analyzed to date.

The aim of the present study was to define MRI criteria from a large series of DSPAs that may help to predict the probability of descent of SDTC during a standard transsphenoidal approach and requirement for extended approaches or second surgery.

Methods

A multicenter retrospective cohort analysis of patients with dumbbell-shaped pituitary macroadenomas operated on via a standard endoscopic transnasal transsphenoidal approach between 2011 and 2020 was conducted. Patient recruitment was performed at two tertiary care centers with expertise in endoscopic skull base surgery (Medical University of Vienna and Keck School of Medicine, University of Southern California).

The inclusion criteria were pituitary macroadenomas with suprasellar extension and a smaller diameter at the level of the diaphragmal opening than at the level of the SDTC (dumbbell-shaped) in both the coronal and sagittal planes (Fig. 1). Patient data and imaging were retrieved from institutional records. Endocrine pituitary function was evaluated by measuring serum blood levels.

This study was approved by institutional ethics committees at both institutions and was performed in accordance with the principles of the Declaration of Helsinki.

Radiological Assessment

On preoperative T1-weighted contrast-enhanced MRI acquired for intraoperative neuronavigation,[13,14] the dumbbell shape of the adenoma was assessed by the following parameters. 1) The maximum tumor diameter was defined as the maximum adenoma diameter at the level of the IDTC and SDTC on coronal or sagittal MRI. 2) The minimum neck diameter was defined as the smallest adenoma diameter at the level of the diaphragmal opening on coronal or sagittal MRI. 3) The neck area (i.e., the smallest area of the diaphragmal opening) was calculated from the two neck diameters by using the approximation formula: $A_{neck} = (diameter_{coronal}/2) \times (diameter_{sagittal}/2) \times \pi$. 4) Total tumor height and individual heights of the SDTC and IDTC were assessed on coronal and sagittal planes orthogonal to the neck diameters. Suprasellar grading was classified according to Hardy and Vezina.[15] 5) Maximum tumor width was assessed on coronal and sagittal planes from the SDTC and IDTC diameters. Furthermore, the largest area of the SDTC was calculated from the two SDTC width diameters by $A_{SDTC} = (diameter_{coronal}/2) \times (diameter_{sagittal}/2) \times \pi$. 6) The neck-to-dome ratio was calculated from the diameters and areas (maximum at dome and minimum at neck), respectively. 7) Tumor volumes of the SDTC and IDTC and total adenoma volume were calculated from semiautomated segmentation of volumetric

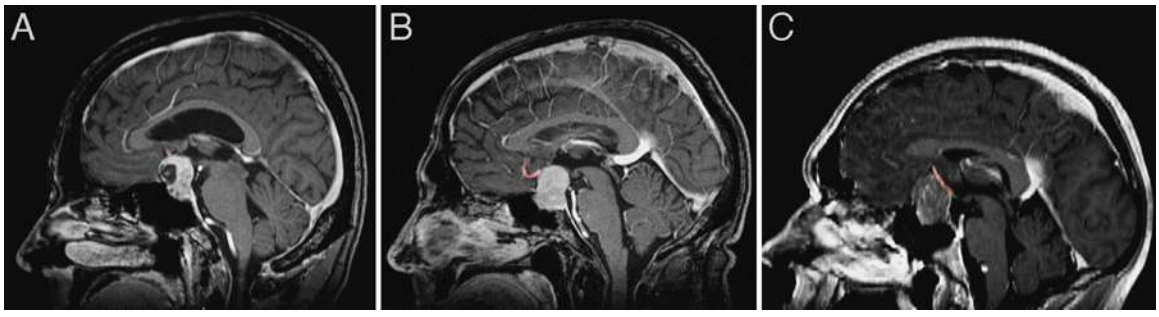

FIG. 2. Sagittal MR images showing the location of the AComA complex (shaded in *red*) in relation to the DSPA. AComA located on the top (**A**), anteriorly (**B**), and posteriorly (**C**) in relation to DSPA tumor extension. Figure is available in color online only.

MRI using dedicated software (Synapse3D, Fujifilm; and StealthStation S7, Medtronic). 8) The relation of the SDTC to the anterior communicating artery (AComA) complex was classified as none, contact and exact location of contact (anterior, top, or posterior of the adenoma; Fig. 2), partial encasement, or complete encasement. 9) Contrast uptake was classified as homogeneous or heterogeneous as a measure for tumor texture. Furthermore, the SDTC was assessed as cystic or not. 10) Invasiveness into dura, bone, or compartments of the cavernous sinus (Knosp grade 3 or 4)[16,17] was based on a neuroradiologist's interpretation of the preoperative MRI studies.

Surgical Assessment

The intraoperative behavior of the SDTC (i.e., the main outcome parameter) was binary classified according to the downward herniation of the sellar diaphragm (arachnoid layer) as descending (group A) versus not or incompletely/asymmetrical descending (group B). The postoperative residual SDTC was assessed on postoperative neuroimaging, with the exception of early reoperation. The adenoma consistency was classified as soft or fibrous by the performing neurosurgeon.[10,18] In contrast to soft suckable adenoma tissue, fibrous tumor components were defined of stiff consistency with septated tumor matrix that was unsuckable and difficult to resect with curettes. Invasiveness into dura, bone or cavernous sinus was judged intraoperatively by the neurosurgical team through direct endoscopic visualization.

Histopathological Assessment

Postoperative histopathological examination was performed by the local neuropathologists according to the latest World Health Organization criteria. Hormone expression was assessed based on immunohistochemical-stained paraffin-embedded tissue sections. Cell proliferation was assessed using immunohistochemical staining for Ki-67 and was quantified by counting 1000 cells in the hot spot area.

Postoperative Outcome

According to the intraoperative behavior of the SDTC, the number of cases with postoperatively increased SDTC volume and/or neurological deterioration due to hemorrhagic transformation of the adenoma remnants with the requirement for emergency transcranial surgery was assessed. The following additional intra- and postoperative complications were evaluated according to the meta-analysis by Ammirati et al.:[19] death, vascular complications (internal carotid artery injury), visual loss, meningitis, postoperative CSF leak, epistaxis, sinusitis, diabetes insipidus (permanent or temporary), anterior pituitary insufficiency, and hyponatremia.

Extent of resection was assessed on follow-up imaging as gross-total resection (GTR), subtotal resection (80%–99%), or partial resection (< 80%); the respective location of the adenoma remnant; and further treatments.[20] Postoperative imaging included an early CT scan within the first 3 postoperative days followed by routine 3-month and 1-year MRI controls. In functioning adenomas, the latest consensus statements for endocrine remission were employed.[21]

Statistical Analysis

The data are presented as mean (range) for continuous variables and as frequencies for categorical variables. To analyze differences between group A (tumor descent) and group B (tumor nondescent), a chi-square test with Pearson's correlation coefficient was performed. Differences in continuous variables between the two groups were assessed using unpaired t-tests.

To assess potential prognostic variables for intraoperative tumor descent/nondescent, we evaluated the following: maximum size, maximum height (supra- and infradiaphragmal), maximum width (supra- and infradiaphragmal), area (diaphragm and SDTC), tumor volume (total, supra-, and infradiaphragmal), and neck-to-dome ratio (diameter and area). Significant variables of these were tested using a binary logistic regression analysis. Receiver operating characteristic (ROC) curve analysis was performed to evaluate the diagnostic power of significant variables in discriminating between groups and find a possible cutoff value to predict an intraoperative tumor descent. A two-sided p value < 0.05 was considered statistically significant. For statistical analyses, IBM SPSS version 25.0 software (IBM Corp.) was used.

Results

Patient Characteristics

The study cohort consisted of 99 patients (Medical Uni-

TABLE 1. Patient and tumor histopathological characteristics

	DSPA Series
Patient characteristics	
No. of patients	99
1st op	89 (90)
Reop	10 (10)
Mean age, yrs	55.7 (18–81)
≤65	70 (71)
>65	29 (29)
Female/male sex	1:2
Mean follow-up, yrs	2.6 (0.6–10)
Tumor characteristics	
Functional classification	
Functional	4 (4)
Nonfunctional	95 (96)
WHO 2017 classification	
Somatotroph	1 (1)
Lactotroph	2 (2)
Mammosomatotroph	
Thyrotroph	
Corticotroph	7 (7)
Gonadotroph	66 (67)
Null cell	21 (21)
Plurihormonal	2 (2)
Consistency	
Soft	74 (75)
Fibrous	25 (25)
Invasiveness (direct endoscopic visualization)	23 (23)
Mean Ki-67, %	3.9 (0.6–14)

Values represent the number of patients (%) or mean (range) unless stated otherwise.

versity of Vienna and Keck School of Medicine, University of Southern California, combined). The mean patient age was 55.7 years (range 18–81 years); 33 patients (33%) were female, and 66 patients (67%) were male (Table 1). Initial symptoms were bitemporal visual field cut (93/99 patients, 94%), visual acuity loss (79/99 patients, 80%) and headache (76/99 patients, 77%). The preoperative endocrine workup revealed hypopituitarism in more than one axis in 14 patients (14%) and hormonal overproduction in 4 patients. Overall, 95 patients (96%) had nonfunctioning pituitary adenomas (96%), and 4 patients (4%) had functioning adenomas (2 lactotroph adenomas, 1 somatotroph adenoma, and 1 corticotroph adenoma).

Radiological Assessment

On preoperative MRI, all DSPAs were macroadenomas (maximum tumor diameter 33 mm, range 17–71 mm; and volume 13 cm^3, range 2–88 cm^3) (Table 2). DSPAs with intraoperative descent (group A) had a significantly smaller diameter than DSPAs that did not descend (group B, 30 vs 42 mm, $p < 0.001$). Furthermore, group A DSPAs had a significantly smaller volume than group B DSPAs (10 vs 22 cm^3, $p < 0.001$). Overall, the SDTC was significantly larger than the IDTC (diameter 19 vs 16 mm, $p < 0.001$; and volume 7.5 vs 5.6 cm^3, $p = 0.007$). Furthermore, within groups A and B, the SDTC was significantly larger than the IDTC (group A: size $p < 0.001$, volume $p = 0.031$; and group B: size $p = 0.006$, volume $p = 0.046$).

Comparison between the groups revealed significantly larger mean SDTC and IDTC in group B than in group A (SDTC 24 vs 17 mm, $p < 0.001$ and volume 13.5 vs 5.3 cm^3, $p < 0.001$; IDTC 19 vs 15 mm, $p = 0.001$ and volume 8.7 vs 4.5 cm^3, $p < 0.001$). The mean diameter at the bottleneck or waist of the diaphragma sellae was 17 mm (range 5–32 mm), and the corresponding area of the diaphragmal opening was 256 mm^2 (range 17–891 mm^2) with no significant differences between groups A and B (diameter 17 vs 17.5 mm, $p = 0.607$; and area 242 vs 296 mm^2, $p = 0.093$).

The ratio of the diaphragmal opening to the suprasellar tumor component (neck-to-dome ratio) was 1.3 (range 1.1–2.6) for diameter and 2.0 (range 1.1–6.5) for the area. The neck-to-dome ratio was significantly lower in group A than in group B (diameter 1.3 vs 1.5 mm, $p < 0.001$; and area 1.7 vs 2.7, $p < 0.001$).

Involvement of the AComA complex was encountered in 61 DSPAs (62%); the remaining 38 DSPAs (38%) were distant to the AComA complex. Mere contact with the AComA was observed in 48 DSPAs (48%); this contact occurred at the top of the tumor in 46%, anteriorly in 33%, and posteriorly in 21% to the AComA complex. Partial or complete encasement of the AComA complex was evident in 12 DSPAs (12%) and 1 DSPA (1%), respectively.

Logistic regression analysis revealed the neck-to-dome area ratio ($p < 0.001$), the width of the suprasellar component ($p = 0.003$), the height of the DSPA ($p = 0.016$), the neck-to-dome diameter ratio ($p = 0.026$), and the height of the suprasellar tumor component ($p = 0.047$) as significant factors for intraoperative tumor nondescent.

For neck-to-dome area ratio, ROC analysis revealed an area under the curve of 0.75 (95% CI 0.63–0.87). At a cutoff level of 1.9, the sensitivity and specificity for tumor nondescent were 77% and 34%, respectively (Fig. 3).

Surgical Assessment

Patients in both centers were operated on via a pure direct endoscopic approach; an extended approach was not used in any of the patients in the study cohort. Tumor descent was found in 73 patients (74%) (group A) and nondescent in 26 patients (26%) (group B) intraoperatively.

The SDTC showed a partial or complete cystic transformation in 28 patients (28%). Intraoperatively, the tumor consistency was soft (grades 1–3) in 74 patients (75%) and fibrous (grades 4 and 5) in 25 patients (25%). A fibrous tumor consistency was found significantly more often in group B (13/26 50%) than in group A (12/73, 16%) ($p < 0.001$).

Pressure on the optochiasmatic system was found to have resolved in 72 (99%) of the 73 group A patients. In 30 (41%) of these 73 patients, postoperative CT was performed and showed partial bleeding into the tumor cavity in 11 patients (37%), although this is a common finding on initial imaging following pituitary adenoma resection. In 1 patient, although the volume of the suprasellar mass de-

TABLE 2. Neuroimaging assessment

	Overall	Group A (n = 73)	Group B (n = 36)	p Value
Mean max diameter, mm	33 (17–71)	30	42	<0.001
IDTC	16 (7–36)	15	19	0.001
SDTC	19 (9–45)	17	24	<0.001
Mean vol, cm^3	13 (2–88)	10	22	<0.001
IDTC	5.6 (1–24)	4.5	8.7	<0.001
SDTC	7.5 (1–67)	5.3	13.5	<0.001
Mean IDTC-to-SDTC ratio	1.5 (0.2–8)	0.8	1.6	0.048
Mean max diameter width of SDTC, mm	24 (10–55)	22	29	<0.001
Mean width of SDTC area, mm^2	481 (97–2195)	400	710	<0.001
Mean min neck diameter, mm	17.1 (5–32)	16.9	17.5	NS
Mean neck area, mm^2	256.1 (17–891)	242	296	NS
Mean neck-to-dome ratio				
Diameter	1.3 (1–2.6)	1.3	1.5	<0.001
Area	2 (1–6.5)	1.7	2.7	<0.001
Knosp high grade				
3A	23 (23)	17	6	
3B	3 (3)	2	1	
4	4 (4)	0	4	
Suprasellar grading (Hardy-Vezina)[15]				
A	3 (3)	2	1	
B	57 (58)	51	6	
C	28 (28	16	12	
D	11 (11)	4	7	
Position of the AComA				
At top	39 (39)	31	8	
Anterior	47 (48)	33	14	
Posterior	13 (13)	9	4	
Relation to the AComA complex				
None	38 (38)	30	8	
Contact	48 (48)	39	9	
Partial encasement	12 (12)	4	8	
Total encasement	1 (1)	0	1	

NS = not significant.
Values represent the number of patients (%) or mean (range) unless stated otherwise.

creased on postoperative imaging, bleeding into the tumor cavity/tumor remnant caused a decrease in visual acuity on the left side, which led to an early reoperation in this patient. A GTR was achieved in 58 (84%) of 69 patients; 4 patients were lost to long-term follow-up. Reoperation due to growth of the tumor remnant was necessary in 6 patients, and 1 patient underwent Gamma Knife radiosurgery.

In 3 (4%) of the 73 patients in group A, a tumor remnant above the diaphragmal level was found on follow-up MRI. In patients with tumor nondescent (group B), a tumor remnant was found in all patients on postoperative neuroimaging. In comparison with the preoperative SDTC, a mean volume of 5.4 cm^3 (range 1–23 cm^3) was found on postoperative neuroimaging, which corresponds to a mean percentage of 38% (range 16%–65%) of remaining tumor mass.

Early reoperation due to a hemorrhagic transformation of the remaining suprasellar tumor component causing mass effect and neurological deterioration was necessary in 6 (23%) of the 26 patients in group B (Fig. 4). In the remaining 20 patients, the tumor descended into the IDTC in 14 patients (70%) (Fig. 5). A further reoperation in the long-term follow-up was necessary in 4 patients, and Gamma Knife radiosurgery in 6 patients.

Histopathological Assessment

The most common tumor subtype in the patient cohort was gonadotroph adenomas (67%), followed by null-cell adenomas (21%) (Table 1). Functioning macroadenomas were predominantly found in group A (3 of 4 patients), with lactotroph adenomas being the most common subgroup (2 of 4 patients). The analysis of the Ki-67 (MIB-1)

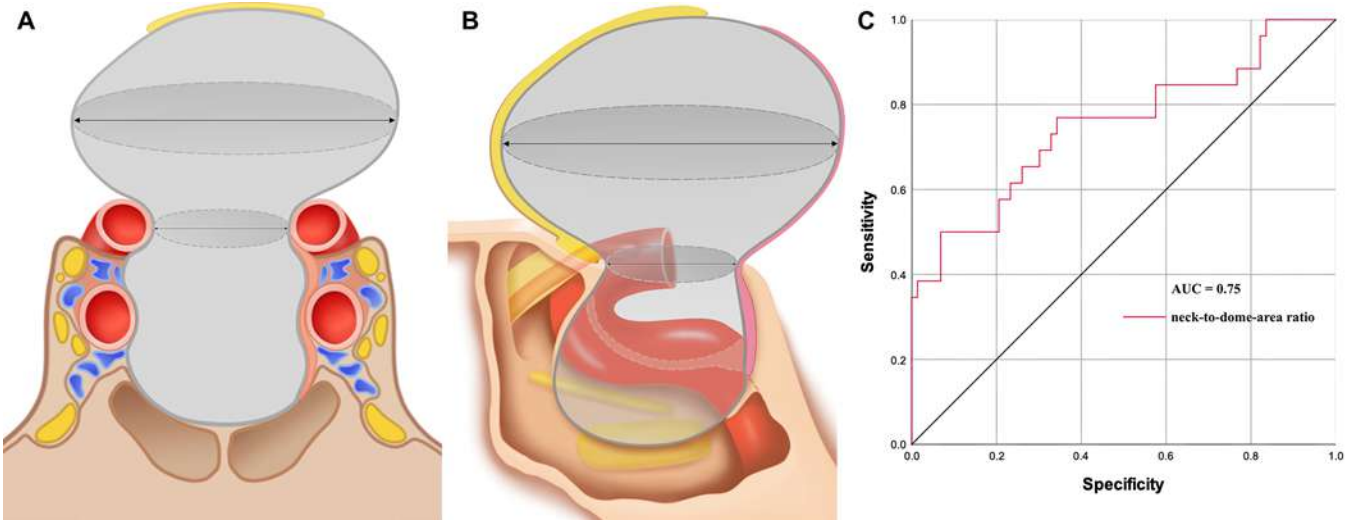

FIG. 3. A and B: Illustrations in the coronal (A) and sagittal (B) planes demonstrating measurements of neck and dome area. **C:** ROC analysis showing the diagnostic strength of neck-to-dome area ratio with respect to tumor descent. Figure is available in color online only.

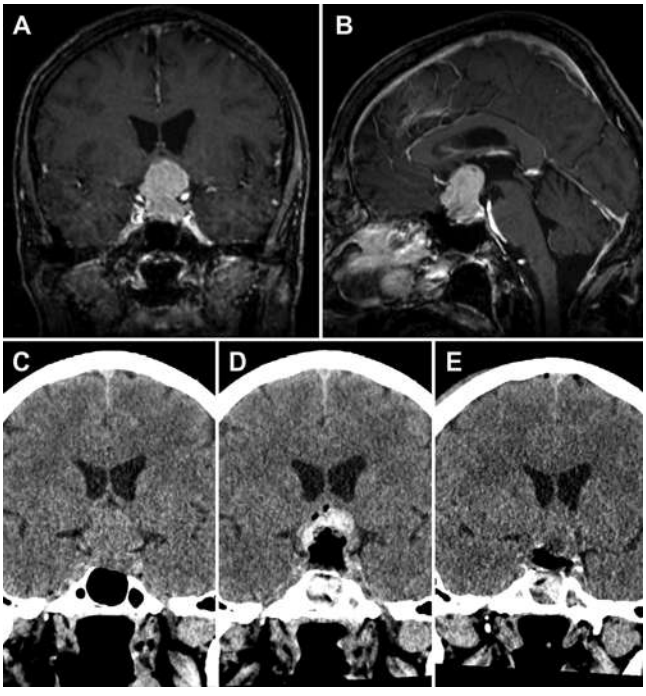

FIG. 4. Postoperative hemorrhagic transformation of the remaining suprasellar tumor component. MRI (A and B) and CT (C–E) sequences obtained in a patient with postoperative deterioration and early transcranial surgery. **A:** Coronal view of the DSPA with displacement of the third ventricle. **B:** Sagittal view of the DSPA. **C:** CT scan obtained preoperatively showing tumor extension. **D:** Postoperative image obtained immediately after endoscopic endonasal transsphenoidal surgery, showing a hemorrhagic transformation of the suprasellar tumor remnant. **E:** Postoperative image obtained after early transcranial surgery before transferring the patient to the ICU.

level revealed a mean value of 3.9 (range 0.6–14) with no statistically significant difference between groups (range 3.3 vs 3.4) ($p = 0.627$).

Postoperative Outcome

Overall, vision improved postoperatively in 59 patients (60%), remained stable in 38 patients (38%), and worsened in 2 patients (2%). The visual field improved in 62 patients (63%), remained stable in 35 patients (35%), and worsened in 2 patients (2%).

Within the cohort, no patient died due to surgery. A hemorrhagic transformation of the tumor remnant occurred in 7 (7%) of the 99 patients, necessitating an acute intervention via a transcranial subfrontal approach (group A: 1 patient, group B: 6 patients; $p < 0.001$). An intraoperative CSF leak was significantly more present in patients in group B (19/26, 73%) than those in group A (31/73, 43%) ($p = 0.007$). Furthermore, severe morbidity included loss of vision/distinct worsening in 2 patients (2%), permanent cranial nerve palsy in 4 patients (4%, all cranial nerve III), meningitis in 1 patient (1%), postoperative CSF leaks in 9 patients (9%), permanent diabetes insipidus in 1 patient (1%), and new postoperative anterior pituitary insufficiency in 13 patients (13%) (Table 3).

Discussion

Preoperative knowledge about the possibility to completely resect DSPAs via a direct transnasal approach is important for considerations of the individual treatment strategy. In the present multicenter study of 99 patients with DSPA, we therefore identified neuroimaging features that are predictive for intraoperative tumor descent. Overall, the neck-to-dome area ratio remained the primary predictor for supradiaphragmal tumor nondescent.

For application in the routine clinical setting, we propose the following approximation formula for tumor nondescent: (supradiaphragmal diameter$_{coronal}$ × supradia-

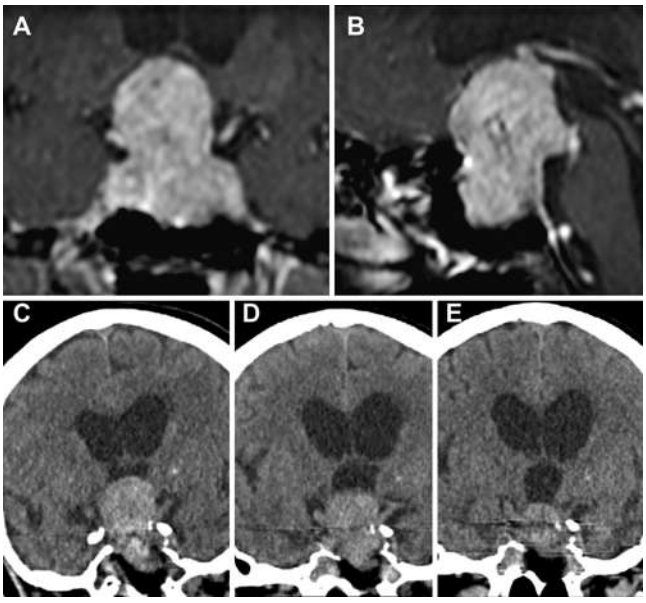

FIG. 5. Tumor nondescending intraoperatively; conservative management and wait for descent. MRI (A and B) and CT (C–E) sequences obtained in an elderly patient with preoperatively hydrocephalic configurated ventricular system. **A:** Coronal view of the DSPA, with displacement of the third ventricle. **B:** Sagittal view of the DSPA. **C:** Postoperative imaging obtained 2 days after ETS showing a hemorrhagic transformation of remaining tumor remnant. **D:** Postoperative image obtained 11 days after tumor resection depicting tumor descent. **E:** Postoperative image obtained 25 days after tumor resection, depicting further tumor degradation.

phragmal diameter$_{sagittal}$)/(neck diameter$_{coronal}$ × neck diameter$_{sagittal}$) ≥ 2.

Potential Factors for DSPA Growth

In general, tumors enlarge along paths of least resistance.[22] Except for somatotroph adenomas, macroadenomas most commonly expand into the suprasellar space through the diaphragmatic aperture in up to 80% of cases.[23] The diaphragm that forms the roof of the sella turcica is composed of a double-layer fold of dura mater pierced by an opening in its center transmitting the pituitary stalk.[24–26] However, the characteristics of this opening are highly variable. From 20 cadaver heads, Campero et al. reported mean diaphragm aperture diameters of 7 mm (range 3–11 mm) in the anteroposterior direction (tuberculum sellae to dorsum sellae) and 7 mm (range 3–14 mm) in the lateral-lateral direction (cavernous sinus to cavernous sinus).[27] They stratified the results into three groups: < 4 mm in 20%, 4–8 mm in 40%, and > 8 mm in 40%. Their findings were confirmed by MRI-based studies.[28,29] This variability in the diameter of the diaphragmal opening likely explains the variable neck diameter in pituitary adenomas that extend into the suprasellar space and consequently the dumbbell shape.[30,31]

Of note, our results revealed that the mean diaphragmal opening diameter showed no statistically significant difference between the tumor descent and nondescent groups. However, in tumors that showed no descent of the suprasellar component despite methods of increasing the intracranial pressure, the neck-to-dome area ratio played a crucial role to predict tumor nondescent. This is of interest, as the suprasellar remnant carries the risk of hemorrhagic transformation due to an induced hypoxia and rupture of immature tumor vessels.[12,32] Other anatomical factors, such as contact with the AComA complex, except for a complete encasement of the vessels, showed no correlation with a nondescent. Male preponderance (twofold) and predominance of nonfunctioning adenomas (96%) may be additional biological factors of DSPA occurrence.

Therapeutic Options of Potentially Nondescending DSPAs

The direct endonasal endoscopic approach resulted in an overall GTR rate of 84% in our multicenter study. A suprasellar tumor remnant was found in all patients with incomplete resections. In case of a supradiaphragmal adenoma remnant, hemorrhagic transformation was observed (37%) and prompted for a subfrontal approach for chiasmal decompression in 7 patients (7%). Therefore, we advise for early neuroimaging and reoperation in case of mass effect or neurological deterioration in DSPA.[6,33–35]

Furthermore, in one of these cases in which the patient had preoperative severe compromised visual function, a direct endoscopic approach resulted in complete amaurosis postoperatively. The optic chiasm was never visible during surgery or on postoperative MRI with the tumor completely removed. We attribute pulling maneuvers when removing the suprasellar adenoma part to this severe complication. As a consequence, our policy was adapted to

TABLE 3. Perioperative complications

	Overall	Group A (n = 73)	Group B (n = 26)
ICA injury	0	0	0
Stroke	0	0	0
Vegetative state	0	0	0
SDTC hemorrhagic transformation (emergency op)	7 (7)	1 (1)	6 (23)
Meningitis	1 (1)	1 (1)	0
Loss of vision or distinct worsening	2 (2)	1 (1)	1 (4)
Permanent cranial nerve palsy			
III	4 (4)	2 (3)	2 (8)
Postop CSF leak	9 (9)	6 (8)	3 (12)
Hydrocephalus requiring shunting	0	0	0
Epistaxis	3 (3)	2 (3)	1 (4)
Sinusitis	1 (1)	0	1 (4)
Permanent new anterior pituitary insufficiency	13 (13)	10 (14)	3 (12)
Diabetes insipidus			
Transient	8 (8)	5 (7)	3 (12)
Permanent	1 (1)	1 (1)	0
Hyponatremia	16 (16)	11 (15)	5 (19)

Values represent the number of patients (%).

wait for a descent of the suprasellar part and follow up on possible tumor regrowth, with the necessity of a delayed second endoscopic endonasal transsphenoidal surgery in 4 patients and radiosurgery in 6 patients.

In addition to the direct endoscopic approach, which was performed in all of our patients, an extended endonasal approach via the transtuberculum/transplanum route may be an option. The goal of this approach is to extracapsularly resect and directly visualize the suprasellar tumor component.[31,36–39] In particular, in patients with a prefixed or stretched optochiasmal complex over the tumor capsule, the extended endonasal approach can preserve neurovascular structures from possibly tractive or direct trauma or retraction of neurovascular structures. In contrast, a primary transcranial approach has the risk of possible harm to the optochiasmal system and is limited in reaching the infradiaphragmal and parasellar tumor components.

The extended endonasal approach, however, is not without limitations. First, the surgical corridor is narrowed by the protuberances of the optic nerves that define the lateral limits. Furthermore, in cases of tumor recurrence, scar tissue formation with adherence to neurovascular structures limits the rate of tumor resection, and an inability to raise a competent vascularized nasoseptal flap increases the risk of CSF leakage. In such cases, a subfrontal approach to remove the supradiaphragmal adenoma component or fractional stereotactic radiosurgery may be considered. Furthermore, the option of an extended endonasal approach depends on the surgeon's experience, tumor consistency, and patient counseling. The proposed approximation formula of neck-to-dome area ratio may serve as an additional tool for treatment options of DSPA.

Limitations

Because of the rarity of DSPAs, the study design was retrospective with its inherent limitations. Applying a multicenter approach, we were able to increase the total case count to 99 consecutive patients. In an effort to keep our data homogenized, we restricted our inclusion criteria to only direct endonasal endoscopic approaches. Although both centers do have ample experience in extended endonasal endoscopic surgery, we can only hypothesize about the option of such an approach for DSPAs. Resultant tumor descent as it pertains to neck-to-dome area on extended endonasal cases warrants future study.

Conclusions

In the present retrospective multicenter study, the neck-to-dome area ratio was found to be of prognostic value for intraoperative tumor nondescent in DSPAs operated on via a direct endonasal endoscopic approach. Despite a possible tumor descent on follow-up images, such a nondescent carried the inherent risk of hemorrhagic transformation in all cases. If nondescent is anticipated from preoperative MRI, the surgeon should be prepared for early second subfrontal decompression or consider an extended approach as the primary option.

References

1. Liu JK, Das K, Weiss MH, Laws ER Jr, Couldwell WT. The history and evolution of transsphenoidal surgery. *J Neurosurg*. 2001;95(6):1083-1096.
2. Cappabianca P, Cavallo LM, de Divitiis E. Endoscopic endonasal transsphenoidal surgery. *Neurosurgery*. 2004;55(4):933-941.
3. Doglietto F, Prevedello DM, Jane JA Jr, Han J, Laws ER Jr. Brief history of endoscopic transsphenoidal surgery—from Philipp Bozzini to the First World Congress of Endoscopic Skull Base Surgery. *Neurosurg Focus*. 2005;19(6):E3.
4. Kanter AS, Dumont AS, Asthagiri AR, Oskouian RJ, Jane JA Jr, Laws ER Jr. The transsphenoidal approach. A historical perspective. *Neurosurg Focus*. 2005;18(4):e6.
5. Solari D, Cavallo LM, Cappabianca P. Surgical approach to pituitary tumors. *Handb Clin Neurol*. 2014;124:291-301.
6. Zada G, Du R, Laws ER Jr. Defining the "edge of the envelope": patient selection in treating complex sellar-based neoplasms via transsphenoidal versus open craniotomy. *J Neurosurg*. 2011;114(2):286-300.
7. Saito K, Kuwayama A, Yamamoto N, Sugita K. The transsphenoidal removal of nonfunctioning pituitary adenomas with suprasellar extensions: the open sella method and intentionally staged operation. *Neurosurgery*. 1995;36(4):668-676.
8. Matsuyama J, Kawase T, Yoshida K, Hasegawa M, Hirose Y, Nagahisa S, et al. Management of large and giant pituitary adenomas with suprasellar extensions. *Asian J Neurosurg*. 2010;5(1):48-53.
9. Ko HC, Lee SH, Shin HS, Koh JS. Predicting arachnoid membrane descent in the chiasmatic cistern in the treatment of pituitary macroadenoma. *J Korean Neurosurg Soc*. 2021;64(1):110-119.
10. Rutkowski MJ, Chang KE, Cardinal T, Du R, Tafreshi AR, Donoho DA, et al. Development and clinical validation of a grading system for pituitary adenoma consistency. *J Neurosurg*. 2021;134(6):1800-1807.
11. Alleyne CH Jr, Barrow DL, Oyesiku NM. Combined transsphenoidal and pterional craniotomy approach to giant pituitary tumors. *Surg Neurol*. 2002;57(6):380-390.
12. Micko A, Agam MS, Brunswick A, Strickland BA, Rutkowski MJ, Carmichael JD, et al. Treatment strategies for giant pituitary adenomas in the era of endoscopic transsphenoidal surgery: a multicenter series. *J Neurosurg*. Published online August 13, 2021; doi:10.3171/2021.1.JNS203982
13. Micko A, Hosmann A, Marik W, Bartsch S, Weber M, Knosp E, Wolfsberger S. Optimizing MR imaging for intraoperative image guidance in sellar pathologies. *Pituitary*. 2020;23(3):266-272.
14. Micko A, Hosmann A, Wurzer A, Maschke S, Marik W, Knosp E, Wolfsberger S. An advanced protocol for intraoperative visualization of sinunasal structures: experiences from pituitary surgery. *J Neurosurg*. 2020;133(1):240-248.
15. Hardy J, Vezina JL. *Transsphenoidal Neurosurgery of Intracranial Neoplasm*. Vol 15. Raven Press; 1976.
16. Micko A, Oberndorfer J, Weninger WJ, Vila G, Höftberger R, Wolfsberger S, Knosp E. Challenging Knosp high-grade pituitary adenomas. *J Neurosurg*. 2019;132(6):1739-1746.
17. Micko AS, Wöhrer A, Wolfsberger S, Knosp E. Invasion of the cavernous sinus space in pituitary adenomas: endoscopic verification and its correlation with an MRI-based classification. *J Neurosurg*. 2015;122(4):803-811.
18. Woodworth GF, Patel KS, Shin B, Burkhardt JK, Tsiouris AJ, McCoul ED, et al. Surgical outcomes using a medial-to-lateral endonasal endoscopic approach to pituitary adenomas invading the cavernous sinus. *J Neurosurg*. 2014;120(5):1086-1094.
19. Ammirati M, Wei L, Ciric I. Short-term outcome of endoscopic versus microscopic pituitary adenoma surgery: a systematic review and meta-analysis. *J Neurol Neurosurg Psychiatry*. 2013;84(8):843-849.
20. Cappabianca P, Cavallo LM, Colao A, de Divitiis E. Surgical

complications associated with the endoscopic endonasal transsphenoidal approach for pituitary adenomas. *J Neurosurg*. 2002;97(2):293-298.
21. Micko ASG, Wöhrer A, Höftberger R, Vila G, Marosi C, Knosp E, Wolfsberger S. MGMT and MSH6 immunoexpression for functioning pituitary macroadenomas. *Pituitary*. 2017;20(6):643-653.
22. Ramakrishnan VR, Suh JD, Lee JY, O'Malley BW Jr, Grady MS, Palmer JN. Sphenoid sinus anatomy and suprasellar extension of pituitary tumors. *J Neurosurg*. 2013;119(3):669-674.
23. Zada G, Lin N, Laws ER Jr. Patterns of extrasellar extension in growth hormone-secreting and nonfunctional pituitary macroadenomas. *Neurosurg Focus*. 2010;29(4):E4.
24. Renn WH, Rhoton AL Jr. Microsurgical anatomy of the sellar region. *J Neurosurg*. 1975;43(3):288-298.
25. Busch W. Morphology of sella turcica and its relation to the pituitary gland. Article in German. *Virchows Arch Pathol Anat Physiol Klin Med*. 1951;320(5):437-458.
26. Rhoton AL Jr. The sellar region. *Neurosurgery*. 2002;51(4)(suppl):S335-S374.
27. Campero A, Martins C, Yasuda A, Rhoton AL Jr. Microsurgical anatomy of the diaphragma sellae and its role in directing the pattern of growth of pituitary adenomas. *Neurosurgery*. 2008;62(3):717-723.
28. Nomura M, Tachibana O, Yamashima T, Yamashita J, Suzuki M. MRI evaluation of the diaphragmal opening: using MRI parallel to the transsphenoidal surgical approach. *J Clin Neurosci*. 2002;9(2):175-177.
29. Tsutsumi S, Ono H, Yasumoto Y, Ishii H. The diaphragma sellae, diaphragm opening, and subdiaphragmatic cistern: an anatomical study using magnetic resonance imaging. *Surg Radiol Anat*. 2019;41(5):529-534.
30. Ferreri AJ, Garrido SA, Markarian MG, Yañez A. Relationship between the development of diaphragma sellae and the morphology of the sella turcica and its content. *Surg Radiol Anat*. 1992;14(3):233-239.
31. Di Maio S, Cavallo LM, Esposito F, Stagno V, Corriero OV, Cappabianca P. Extended endoscopic endonasal approach for selected pituitary adenomas: early experience. *J Neurosurg*. 2011;114(2):345-353.
32. Semple PL, Jane JA, Lopes MB, Laws ER. Pituitary apoplexy: correlation between magnetic resonance imaging and histopathological results. *J Neurosurg*. 2008;108(5):909-915.
33. Sinha S, Sharma BS. Giant pituitary adenomas—an enigma revisited. Microsurgical treatment strategies and outcome in a series of 250 patients. *Br J Neurosurg*. 2010;24(1):31-39.
34. Mortini P, Barzaghi R, Losa M, Boari N, Giovanelli M. Surgical treatment of giant pituitary adenomas: strategies and results in a series of 95 consecutive patients. *Neurosurgery*. 2007;60(6):993-1004.
35. Leung GK, Law HY, Hung KN, Fan YW, Lui WM. Combined simultaneous transcranial and transsphenoidal resection of large-to-giant pituitary adenomas. *Acta Neurochir (Wien)*. 2011;153(7):1401-1408.
36. Solari D, D'Avella E, Bove I, Cappabianca P, Cavallo LM. Extended endonasal approaches for pituitary adenomas. *J Neurosurg Sci*. 2021;65(2):160-168.
37. Cappabianca P, Cavallo LM, Esposito F, De Divitiis O, Messina A, De Divitiis E. Extended endoscopic endonasal approach to the midline skull base: the evolving role of transsphenoidal surgery. *Adv Tech Stand Neurosurg*. 2008;33:151-199.
38. Zhao B, Wei YK, Li GL, Li YN, Yao Y, Kang J, et al. Extended transsphenoidal approach for pituitary adenomas invading the anterior cranial base, cavernous sinus, and clivus: a single-center experience with 126 consecutive cases. *J Neurosurg*. 2010;112(1):108-117.
39. Laufer I, Anand VK, Schwartz TH. Endoscopic, endonasal extended transsphenoidal, transplanum transtuberculum approach for resection of suprasellar lesions. *J Neurosurg*. 2007;106(3):400-406.

Disclosures

Dr. Wolfsberger is currently an educational consultant for Medtronic Surgical Technologies.

Author Contributions

Conception and design: Zada, Micko, Wolfsberger. Acquisition of data: Micko, Keritam, Marik, Strickland, Briggs, Shahrestani, Cardinal. Analysis and interpretation of data: Micko, Wolfsberger. Drafting the article: Micko. Critically revising the article: Zada, Micko, Knosp, Wolfsberger. Reviewed submitted version of manuscript: all authors. Approved the final version of the manuscript on behalf of all authors: Zada. Statistical analysis: Micko. Administrative/technical/material support: Marik. Study supervision: Zada, Wolfsberger.

Correspondence

Gabriel Zada: Keck School of Medicine, University of Southern California, Los Angeles, CA. gabriel.zada@med.usc.edu.